Temporal evolution of characteristic length and fractal dimension for a non-Euclidean system

D. Sen, S. Mazumder,* and J. Bahadur
Solid State Physics Division, Bhabha Atomic Research Centre, Mumbai-400 085, India
(Received 2 December 2008; revised manuscript received 17 February 2009; published 30 April 2009)

In order to understand some yet incomprehensible experimental observations on temporal evolution of characteristic length and fractal dimension of a dynamical system, a model simulation has been attempted. It has been shown that the present simulation corroborates well with the trend of the experimentally observed temporal evolutions of fractal dimension and characteristic length during light water hydration of calcium silicates (C_3S and C_2S) and ordinary Portland cement. The dynamical scaling of the scattering functions was found to be valid during hydration, particularly in intermediate and in late stages of hydration process.

DOI: 10.1103/PhysRevB.79.134207 PACS number(s): 64.75.−g

I. INTRODUCTION

Temporal evolution of mesoscopic structures in condensed systems has received a considerable attention in recent years altogether from experimental, computational, and theoretical points of view. This is due to the relevance of this phenomenon in a wide variety of materials including technologically important materials such as cements,[1–3] alloys,[4–15] ceramics,[16–18] xerogels,[19] polymer,[20–25] glasses,[26–37] liquid mixture,[38–44] etc. The new phase formation is an example of first-order phenomenon. This is a highly nonlinear process far from equilibrium. The second phase starts growing in size, after formation, with time and is influenced by several thermodynamical parameters. Most commonly in the limit $t \rightarrow \infty$, phase-forming systems exhibit a self-similar/self-affined growth pattern with dilation symmetry and a scaling phenomenon, i.e., the morphological pattern of the domains at earlier times looks statistically similar to the pattern at later times apart from the global change in scale implied by the growth of the characteristic length scale $L(t)$—a measure of the time-dependent domain size of the new phase.

For a non-Euclidean system,[45] such as hydrating cement paste, understanding the growth of the second phase constitutes an important area of research because porosity, microstructure, interconnectivity, etc., are important properties of the final cement product.

A non-Euclidean object is quantitatively described by its fractal dimension (D_f) and its cutoff lengths. The density-density correlation function $C(r)=N^{-1}\Sigma_{r'}\rho(r')\rho(r+r')$ follows a power-law relation, $C(r) \propto r^{-\alpha}$, where $\alpha=d_E-D_f$. Here, d_E is the embedding Euclidean dimension. Hydrated cement paste has been known to possess non-Euclidean geometry over a wide length scale. Hydration reaction on a fractal network of cement grains eventually gives rise to space-filling effect and interlocking between the cement grains. During the hydration reaction, Calcium silicates, the main constituent of cements, react with water and produce calcium silicate hydrate (C-S-H) gel and calcium hydroxide. The gel constitutes about 60%–70% of the fully hydrated cement paste and is responsible for most of the properties of cement-based materials. The gel, formed during hydration reaction, starts filling the space around and between the cement particles locking the mass together. By this dynamical process of hydration, the fractal morphology of the hydrated mass evolves with time and domains with non-Euclidean geometry gradually get modified toward a consolidated Euclidean mass. The hydration kinetics determines the rate of dynamical evolution of the fractal dimension and the overall characteristic length scale. The kinetics depends on the cement ingredients, cement-to-water ratio, humidity, etc.

New phase formation is a diffusion-controlled process but aspects such as diffusion or random walk in non-Euclidean geometry are not satisfactorily comprehensible yet and need special attention. In Euclidean geometry, it is established that the curvilinear distance $\sqrt{\langle r^2(t)\rangle}$ covered in time t by a random-walk process is proportional to $t^{1/2}$ and the exponent $\frac{1}{2}$ is independent of dimensionality. If it is conjectured that the curvilinear distance covered for a random walk in fractal geometry also behaves as a power law given by $t^{1/2\nu}$, the exact dependence of ν on the fractal geometry is also yet to be established. To understand new phase formation and the evolution of the new phase in non-Euclidean systems, in recent past small-angle neutron-scattering experiments have been performed on cementatious materials.[1–3]

Small-angle scattering is a well-established technique[46,47] to probe mesoscopic density fluctuations in condensed matter. Previously small-angle scattering has been used to investigate the mesoscopic structures of cements[1–3,48,49] and ceramics.[50–52] It is one of the few tools to obtain the quantitative results on fractal objects in a statistical sense. Ultrasmall-angle scattering (USANS) pertains to the measurement of scattering signal at very small wave-vector transfer (q) and deals with density fluctuations at larger length scales (>10 nm; as exists in ceramics and cements). In recent past, real-time USANS investigations[1–3] [using triple-bounce channel-cut crystal-based instrument S-18 at Institut Laue-Langevin (ILL), Grenoble, France] on hydrated paste of tricalcium silicate ($3CaO\cdot SiO_2 \equiv C_3S$), dicalcium silicate ($2CaO\cdot SiO_2 \equiv C_2S$), ordinary Portland cement (OPC), and calcium sulphates were performed. It is worthy to mention that these studies indicated nonuniqueness in the trend of dynamical evolution in these systems. It was shown[1,2] that in case of hydration reaction of calcium silicates (C_3S and C_2S) and OPC with normal light water, the fractal dimension starts increasing just after the onset of the hydration reaction and gradually reaches a plateau. Further, temporal evolution of the square of the characteristic length (L) of the system mimics the trend of evolution of the fractal

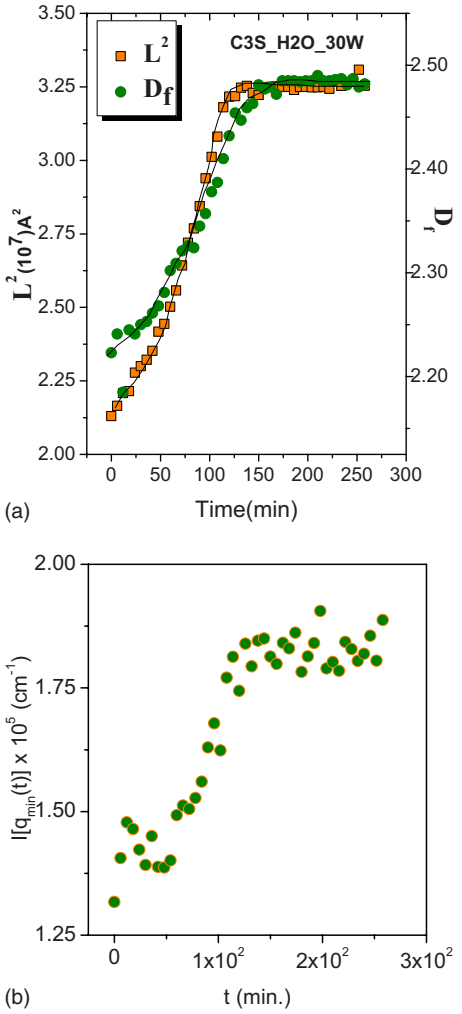

FIG. 1. (Color online) (a). Evolution of fractal dimension and square of the characteristic length with hydration time as observed from the USANS experiments (Ref. 1). We have taken only a typical figure for present presentation. (b). Evolution of USANS intensity at $q \sim 0$ with hydration time (Ref. 1). We have taken only a typical figure for the present presentation.

dimension (D_f) and the same reaches a plateau also and almost at the same time [Fig. 1(a) for C_3S with water-to-cement ratio of 30%]. It is interesting to note that these observations indicate that two physical quantities, characteristic length and fractal dimension, having different dimensionalities (as fractal dimension is a dimensionless quantity while characteristic length has a dimension of length) reach a plateau almost at the similar time and almost in a similar fashion. What remains to be understood is whether the similarity of temporal evolution of altogether two different physical quantities an accidental one. But repeated measurements,[2] varying over wide range of compositions, brought out this phenomenal accidental similarity.

In fact, such incomprehensible observation prompted us to understand the evolution in detail by performing a model simulation. Further, the scattering intensity at the minimum accessible wave-vector transfer [$q=4\pi \sin(\theta)/\lambda$, where 2θ is the scattering angle and λ is the wavelength of the probing neutron] also showed a similar trend [Fig. 1(b)], i.e., it

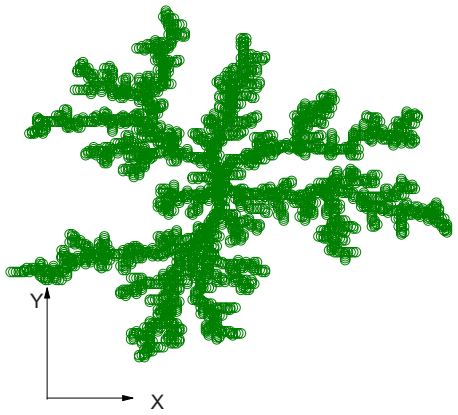

FIG. 2. (Color online) The initial fractal cluster generated using DLA model just at the onset of the hydration.

reaches a plateau after a transient time as shown by fractal dimension and characteristic length. The scattering intensity function showed some kind of scaling behavior with respect to the characteristic length scale $L(t)$. However, in case of the hydration of calcium sulphates,[3] a contrasting behavior was observed. Although the scattering intensity at $q \sim 0$ increases with hydration time and reaches a plateau after some transient time, the fractal dimension and the characteristic length do not show the trend those were observed in the cases of hydration of C_3S, C_2S, or OPC but showed some sinusoidal nature of temporal evolution (see Fig. 2 of Ref. 3). These observations remain quite incomprehensible yet on the basis of linear and nonlinear theories on dynamics of new phase formation for mesoscopic structures in non-Euclidean geometry.

In the present paper, a model simulation has been attempted in order to understand some of the above ultrasmall-angle neutron-scattering experimental observations on dynamical evolution of mesoscopic structure during cement hydration.

II. COMPUTER MODEL AND THE RESULTS ON STRUCTURE EVOLUTION DURING CEMENT HYDRATION

It is well established that during hydration reaction cement particles and C-S-H gel system constitute a non-Euclidean fractal morphology.[16–18,53] For such a system, various physical parameters follow a power-law relation with some other parameters over a wide length scale. The volume $V(r)$ of such an object varies over a wide range of length scale as r^{Df}, where $D_f < 3$. For a normal Euclidean object in three dimensions, the fractal dimension D_f equals to its Euclidean dimension of 3.

A fractal object that is generated using a particular mathematical rule is strictly self-similar and nonrandom in nature. However, for many natural and synthetic objects, the fractals are self-affined (nonidentical scaling constants for various directions) and random in nature. In the last two decades, various computer models have been developed to simulate random fractal objects originated from the agglomeration of the smaller particles. Some of these models are diffusion-

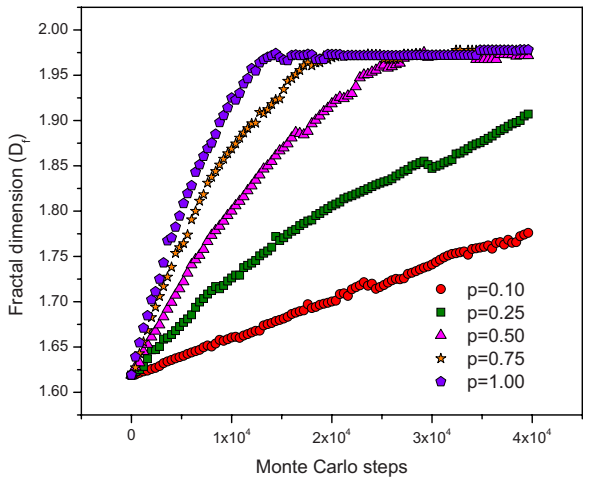

FIG. 3. (Color online) The evolution of fractal dimension (case I) with Monte Carlo steps.

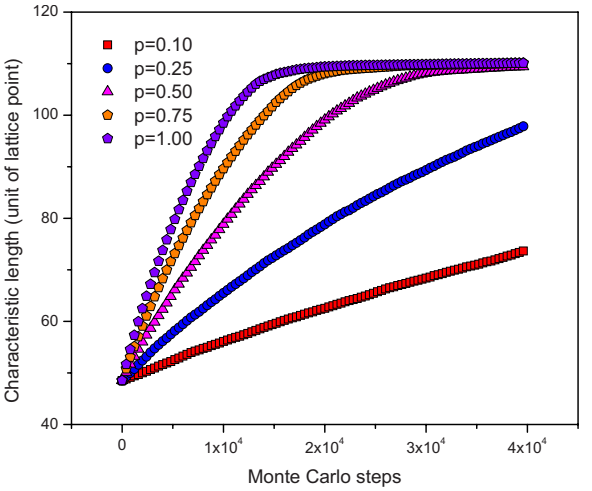

FIG. 4. (Color online) The evolution of characteristic length (case I) with Monte Carlo steps.

limited aggregation (DLA),[54] cluster-cluster aggregation,[55,56] tunable dimension cluster-cluster aggregation,[57,58] and reaction-limited cluster-cluster aggregation.[59] DLA model,[54] one of the first models of these kinds, considers a single seed particle at the origin of a lattice. A second particle is added from a long distance from the origin and undergoes a random walk on the lattice until it reaches a site adjacent to the seed and becomes a part of the growing cluster. Next particle is then introduced at a random distant point and undergoes a random walk until it becomes a part of the growing cluster. The procedure repeats until the desired cluster size is obtained. In this model, a fractal structure can develop during the diffusion-controlled growth and thus provides the motivation toward the choice of this model in many situations. This model has been recognized to be quite well appropriate to describe many dendritic agglomerated structures.

From the real-time USANS experiments, the value of fractal dimension just after the onset of hydration reaction is estimated to be ~2.3. This value of the estimated D_f prompted us to consider the DLA as an initial cluster in order to understand the dynamical evolution of structure. However, to establish that the conclusions of this study do not depend much on this particular choice of morphology, results from a non-DLA cluster will also be presented in the latter portion of this paper. For limitation of available computational resources, the simulation has been restricted in two dimensions only while modeling the evolution of structure during hydration. Figure 2 depicts the initial structure (consisting of 3000 lattice points) obtained with DLA approach. It is noteworthy to mention that the Fractal dimension for a two-dimensional (2D) DLA cluster is ~1.67 and the corresponding Euclidean dimension is 2. Any lattice site for which all nearest-neighbor sites are filled is denoted as a *saturated site* while a site with unfilled neighbors is denoted as an *unsaturated site*. In the next step, the evolution of this structure has been investigated in the light of cement hydration.

The initial DLA structure gets modified because of the onset of the hydration reaction at the available sites. As the time proceeds, the gel fills the available space and, gradually, the structure tends to be a consolidated one. However, the speed of the smoothening process depends on the rate of the reaction kinetics. The present simulation proceeds in the following way. A lattice site on the cluster is chosen at random. The probability for an incoming gel particle to be a part of the existing cluster is considered to be p. If the site is an unsaturated one, then one of the available sites is selected according to the given probability p. In this simulation, the available sites were restricted within a zone of maximum linear extent of the initial cluster. This restriction arises because of the fact that another cluster adjacent to this present cluster will not allow the growth beyond the zone of maximum linear extent of the former cluster. However, for a very diluted system, a growth can occur beyond the maximum extent of a cluster and such situations will be dealt with in the latter part. Once hydration reaction is initiated at one unsaturated site, the new site gets bonded and becomes a part of the existing cluster. The fractal dimension at various instances of the evolving cluster is calculated using box counting method. The evolution of fractal dimension with Monte Carlo steps for different p values is plotted in Fig. 3. It is seen that the fractal dimension increases initially and reaches

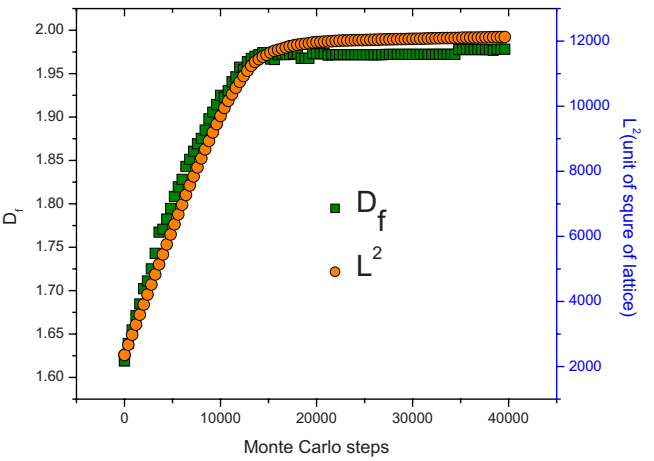

FIG. 5. (Color online) Evolution of the fractal dimension and square of the characteristic length (case I) with Monte Carlo steps.

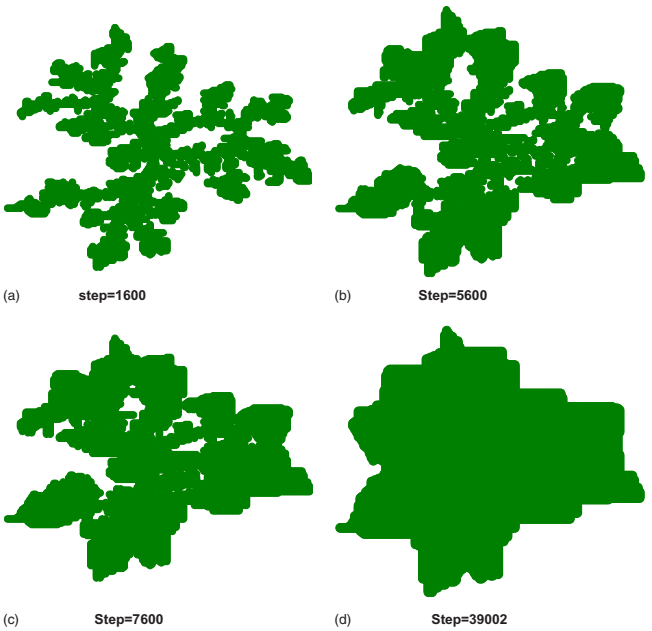

FIG. 6. (Color online) Morphology of the evolving cluster (case I) at different Monte Carlo steps for $p=1$.

a plateau at some time which depends on the deposition probability.

Effective characteristic length was estimated from the square root of the total area of the evolving cluster at any particular instance. It is worthy to mention here that, experimentally, characteristic length $L(t)$ is normally measured using scattering measurements. The scaling hypothesis assumes the existence of a single characteristic length scale $L(t)$ such that the domain sizes and their spatial correlation are time invariant when lengths are scaled by $L(t)$. If there is a signature of interparticle correlation peak in scattering data at a particular wave-vector transfer $(q=q_m)$, then characteristic length is considered to be π/q_m. However, for a polydisperse system there is no universal form for $L(t)$. In some cases,[6–8,13,15,60,61] scaling phenomenon has been observed with $L(t)$ as reciprocal of the first moment of q, i.e., $L(t)=(\frac{\int qI(q,t)dq}{\int I(q,t)dq})^{-1}$. In some other cases,[1–3] scaling phenomenon has been observed with characteristic length, which is square root of the curvature (κ) of the scattering profile at the vicinity of $q\sim 0$, i.e.,

$$\kappa(t) = L^2(t) = \lim_{q\to 0} \frac{|d^2[I(q,t)/I(0,t)]/dq^2|}{(1+\{d[I(q,t)/I(0,t)]/dq\}^2)^{3/2}}.$$

The evolution of the characteristic length L, as obtained from the present simulation, has been depicted in Fig. 4. Similar to the evolution of the fractal dimension D_f, the characteristic length also increases initially and then reaches a plateau depending on the deposition probability.

The functionalities of the evolution of the fractal dimension and the characteristic length are compared in Fig. 5 for $p=1$. Interestingly, it is seen that D_f and L reach plateau at same time. The shapes of the evolving cluster for different Monte Carlo steps for $p=1$ are depicted in Fig. 6. From the figure it is evident that the structure gets more compact with

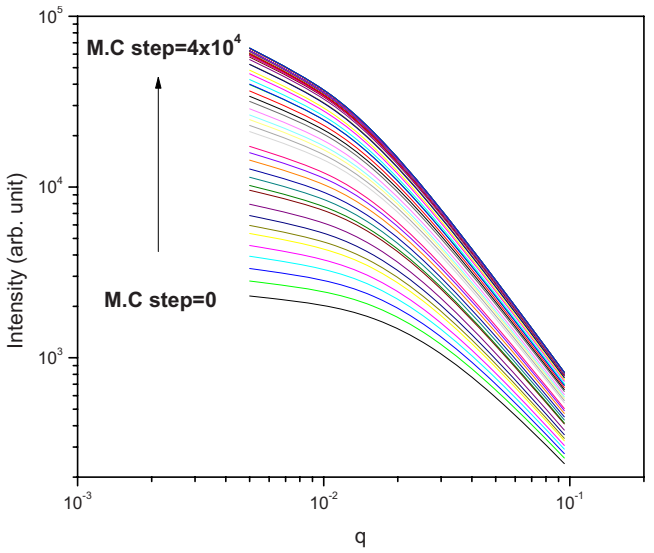

FIG. 7. (Color online) Evolution of the simulated scattering profiles with Monte Carlo steps.

time and also the branching in the initial structure gets smeared out with increase in deposition of gel.

In order to examine the dynamical scaling, the small-angle scattering intensity profile $I(q)$ for the evolving cluster was calculated by the following formula:

$$I(q,t) = CP(q)S(q,t), \tag{1}$$

where C is a scale factor and independent of q; for simplicity $P(q)$ was taken as a form factor of a sphere with radius r_0,

$$P(q) = \frac{[\sin(qr_0) - qr_0\cos(qr_0)]^2}{(qr_0)^6}, \tag{2}$$

and $S(q)$ was taken as that for a mass fractal[62,63]

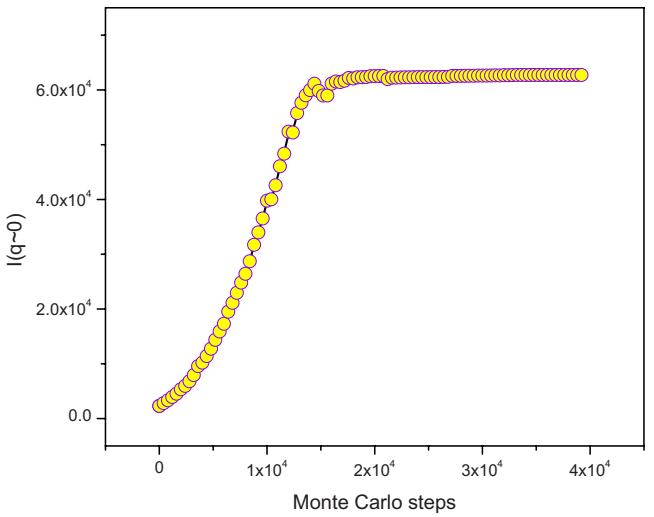

FIG. 8. (Color online) Evolution of simulated scattering intensity at $q\sim 0$.

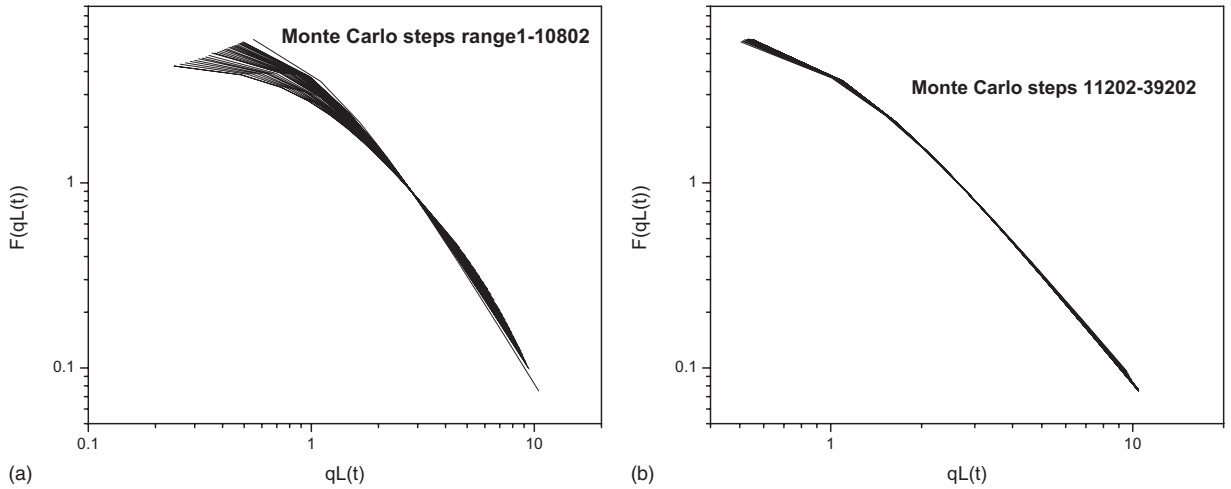

FIG. 9. (a) Normalized scaled structure function for initial stage and (b) scaled structure function for intermediate and late stages.

$$S(q) = 1 + \frac{1}{(qr_o)^{D_f(t)}} \frac{D_f(t)\Gamma[D_f(t)-1]}{\left[1+\frac{1}{q^2\xi^2}\right]^{[D_f(t)-1]/2}} \times \sin\{[D_f(t)-1]\tan^{-1}(q\xi)\}, \quad (3)$$

where ξ is the upper cutoff of the fractal and has been taken same as the characteristic length scale as mentioned above. The simulated scattering profiles are depicted in Fig. 7. The evolution of the scattering intensity at $q \sim 0$ has been depicted in Fig. 8. The normalized function $\tilde{F}[qL(t)]$ was calculated from the following equation:[1–3]

$$\tilde{F}[qL(t)] = \frac{[L(t)]^{-D_f(t)} I(q,t)}{\sum q^{D_f(t)-1} I(q,t)\,\delta q} \quad (4)$$

and plotted in Fig. 9.

In the next step, a situation is considered where the deposition is possible beyond the maximum extent of the initial cluster. Such a situation is expected to occur where the system is diluted enough and the intercluster distance is much larger than the size of each cluster. The evolution of L^2 and D_f in this situation (case II) is depicted in Fig. 10. The evolution of these two parameters both in cases I and II are compared in Figs. 11 and 12, respectively. It is evident that D_f and L^2 evolve quite differently for case II in comparison to case I. The shape of the evolving cluster after long enough time is depicted in Fig. 13. From the figures, it is evident that the evolution of D_f and L^2 and the shape of the evolving cluster differ significantly in case II in comparison to case I. In this case, it is seen that still at large Monte Carlo step (~40 000), there exist sites which are vacant well within the cluster and some sort of branching appears at the periphery.

So far our discussions have been based on evolution considering a DLA-like cluster. However, to establish that the conclusions obtained from the discussions as presented above do not depend much on this particular choice of morphology, simulation has also been performed for an initial non-DLA cluster which is generated by random deposition process on lattice and is somewhat similar to the ballistic deposition[64,65] method. Results from this simulation are presented in Fig. 14.

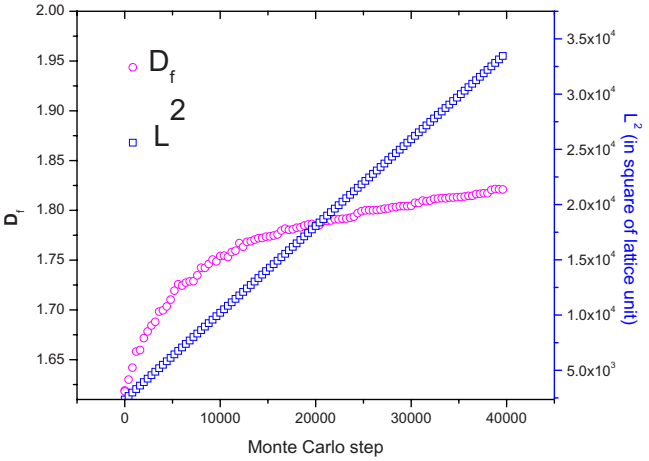

FIG. 10. (Color online) Evolution of D_f and L^2 for case II (see text).

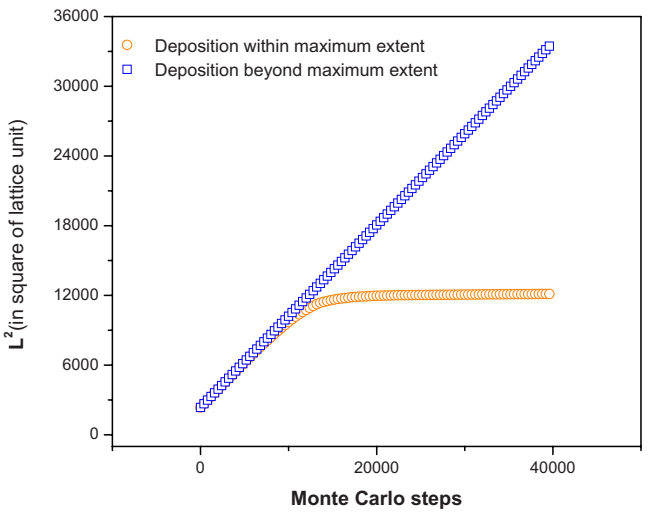

FIG. 11. (Color online) Evolutions of L^2 in cases I and II are compared.

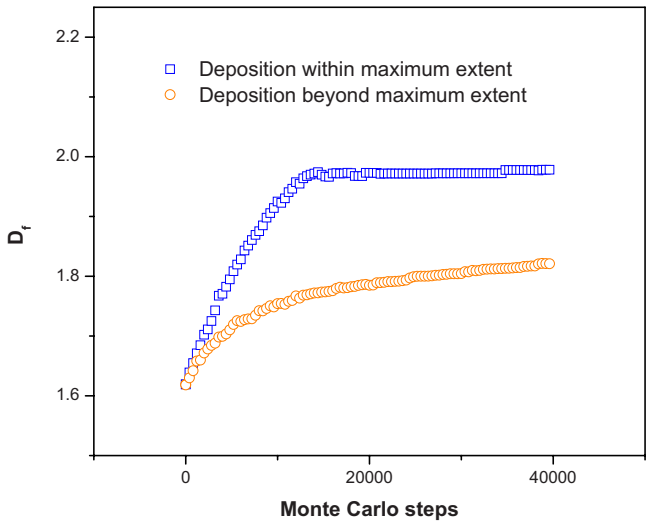

FIG. 12. (Color online) Evolutions of D_f in cases I and II are compared.

The initial structure and the structure after large time (Monte Carlo steps of ~40 000) are depicted in the inset. It is evident from the figure that even in this case, D_f and L^2 reach a plateau at the same instance of time.

III. DISCUSSIONS

From Figs. 3 and 4, it is evident that the onset of hydration reaction in case I leads to a more compact structure and hence enhancement in fractal dimension (D_f) follows. By the deposition of gel, the effective area, vis-à-vis, the characteristic length scale (L) of the cluster increases as well. Both D_f and L increase initially till they reach their corresponding plateau when all the available sites are filled within the cluster.

From Fig. 5, it is evident that the nature of the evolution for D_f and L^2 is almost similar, i.e., both of the parameters initially increase and then reach a plateau at same instance. This corroborates with the trends observed from the USANS experiments on normal light water hydration of C_3S, C_2S, and OPC. Instead of possessing different dimensionalities, two physical quantities, fractal dimension (dimensionless quantity) and characteristic length (having a dimension of length) reach a plateau almost at the same time and almost at same fashion. This may be explained by the fact that the increase in the fractal dimension by the space filling gel occurs within the zone of maximum linear extent (in case I) of a cluster due to the spatial constraint of the adjacent cluster and hence the modification in the fractal dimension is associated with the similar type of modification in characteristic length scale. The evolution of the scattering intensity at $q \sim 0$ also shows the similar trends and reaches a plateau almost at the same value of Monte Carlo steps as shown by D_f and L. The scattering intensity at zero wave-vector transfer ($q=0$) is the product of scattering contrast and the square of the particle volume, i.e, $I(q \sim 0)=(\rho_p-\rho_m)^2V^2$, where ρ_p and ρ_m are the scattering length densities of the particle and the matrix, respectively. At $t \to \infty$, when the characteristic length scale reaches a plateau, $I(q \sim 0)$ also reaches a constant level for a particular contrast value. However, it should be mentioned that in reality the modification in the scattering contrast due to hydration also somewhat modifies the scattering intensity which has not been taken into account in the present simulation.

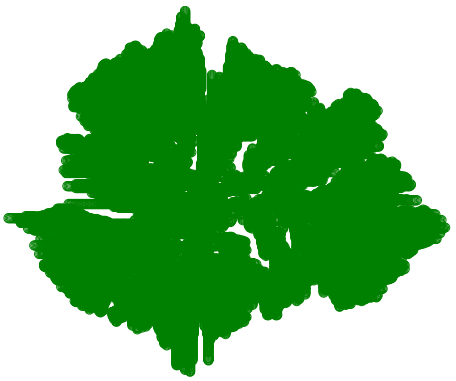

FIG. 13. (Color online) Shape of the evolving cluster in case II after Monte Carlo steps of 40 000.

From Fig. 9(b), it is evident that the present simulation shows that a dynamical scaling behavior of the scattering function holds good in the intermediate and in the late stages as evident from the overlapping of the normalized scaled scattering function for Monte Carlo steps beyond 11 000. However, the dynamical scaling of the scattering function at the initial stage is not as pronounced [Fig. 9(a)] as that has been observed for intermediate and for late stages [Fig. 9(b)].

The results from case II, where deposition proceeds beyond the maximum extent of the initial cluster, will be discussed now. From Figs. 10–12, it has been found that the square of the characteristic length and the fractal dimension in this case behave in different fashion unlike case I. In case II, L^2 keeps on growing (Figs. 10 and 11) because the sites for deposition are always available at least at the boundary of the growing cluster. The growth of the fractal dimension D_f gets somewhat sluggish (Fig. 12) compared to the trend ob-

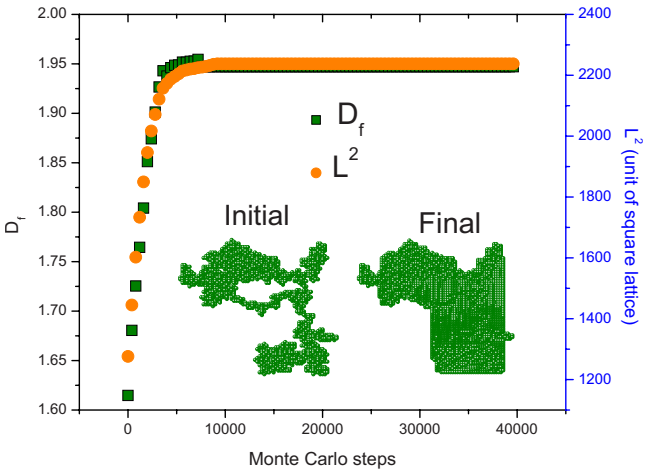

FIG. 14. (Color online) Evolution of D_f and L^2 for a non-DLA cluster for $p=1$. Inset shows the initial and final morphologies of the evolving cluster.

served in case I. This is because of the fact that in such a situation, there is a finite probability of deposition beyond the maximum extent of the initial cluster, which does not give rise to compaction of overall structure unlike case I. However, as the ratio of number of lattices within the maximum extent of initial cluster to the number of available sites for deposition beyond the maximum extent of the initial cluster remains much greater than unity, the rate of compaction, vis-à-vis, the rate of increase in D_f remains somewhat faster initially but growth of D_f slows down gradually as the cluster grows at later stage. It is quite clear that although the rate of increase in D_f decreases with the growth of cluster size, it does not reach a true plateau ever. At this point it is noteworthy to mention that the formation of new phase, i.e., gel, during hydration reaction makes the system to be a nonconserved one. For such system, the modification in fractal dimension depends on the spatial distribution of the new phase. If the spatial constraint of the adjacent clusters exists then it leads to a more compact structure as time passes. However, it is expected that in the absence of spatial constraint, the compaction must depend on the nature of deposition, i.e., whether the deposition is random (like in case II) or a site preferential one where it gives rise to a new branching structure.

It is important to note that the USANS experiments mentioned above were performed on hydrated paste of tricalcium silicate (C_3S) for water-to-cement ratio of 0.3. This ratio of water to cement corresponds to a situation where the cement particles constitute a dense assembly in cement-water matrix. For such a dense system, the available sites for gel deposition during a hydration reaction are bound to be restricted within zone of maximum linear extent of the initial cluster because of the spatial constraints imposed by adjacent clusters. The model described in case I corresponds to such a situation and agrees with the results from USANS experiments. However, for a very diluted system (i.e., when water to cement ratio is very high), growth is not expected to be restricted and is allowed even beyond the maximum extent of a cluster and the model described in case II corresponds to such a situation. It will be worth investigating experimentally, by scattering techniques, whether the D_f and the L^2 reach plateau at different times in case of a very diluted system where the gel deposition is not hindered beyond the maximum extent of the cluster.

It is emphasized that the results presented above do not depend much on this particular choice of morphology of initial cluster. From Fig. 14, it is clear that when the initial cluster is considered different than a DLA cluster and the deposition is allowed within the maximum extent of the initial cluster (similar to case I), D_f and L^2 reach a plateau at the same instance of time.

It is noteworthy that although the above model explains the trend of several experimental observations on hydration of C_3S, C_2S, and OPC, the sinusoidal evolution of the characteristic length and fractal dimension in case of hydration reaction of calcium sulphates is yet to be explained. However, even for the case of hydration of sulphates,[3] the growth of scattering intensity at $q \sim 0$ follows a trend that corroborates with the present simulation.

IV. CONCLUSIONS

Monte Carlo based model simulation showed that the temporal evolution of the fractal dimension of non-Euclidean cluster of hydrated cement paste proceeds by space-filling effect of the C-S-H gel during hydration reaction. The model corroborates well with the temporal of evolution of the fractal dimension and the characteristic length as observed by USANS measurements on calcium silicates (C_3S and C_2S) and OPC. Further, it also supports the appearance of plateau for the above physical quantities nearly at the same time during hydration when the gel deposition is spatially constrained within the maximum extent of the initial cluster. The dynamical scaling of the scattering functions is more pronounced at intermediate and in late stages of hydration reaction than that at initial stage. It would be nice to verify experimentally by scattering techniques whether the fractal dimension and the square of the characteristic length reach plateau at different times in case of a very diluted system where the gel deposition is not hindered beyond the maximum extent of the cluster (as predicted in case II of this paper). Although the present simulation deals with a two-dimensional network, in the next step in the near future, consideration of the three-dimensional network will be attempted within limited computational limitations. More experimental investigations on dynamical evolution of the mesoscopic structure in a non-Euclidean system and the scaling behavior of the scattering functions during hydration reaction are also called for. The present study indicates that the mesoscopic structural kinetics and the phenomenon of dynamical scaling in non-Euclidean systems should be brought into closer scrutiny for various systems in future in order to approach a unique evolution model for dynamical growth of non-Euclidean systems in general and also for the understanding of hydration dynamics in cements in particular.

ACKNOWLEDGMENTS

The authors are grateful to the reviewers for their kind suggestions to improve the quality of presentation.

*smazu@barc.gov.in

[1] S. Mazumder, D. Sen, A. K. Patra, S. A. Khadilkar, R. M. Cursetji, R. Loidl, M. Baron, and H. Rauch, Phys. Rev. Lett. **93**, 255704 (2004).

[2] S. Mazumder, D. Sen, A. K. Patra, S. A. Khadilkar, R. M. Cursetji, R. Loidl, M. Baron, and H. Rauch, Phys. Rev. B **72**, 224208 (2005).

[3] S. Mazumder, R. Loidl, and H. Rauch, Phys. Rev. B **76**, 064205 (2007).

[4] M. Hennion, D. Ronzaud, and P. Guyot, Acta Metall. **30**, 599

(1982).
[5] S. Komura, K. Osamura, H. Fujii, and T. Takeda, Phys. Rev. B **30**, 2944 (1984).
[6] S. Katano and M. Iizumi, Phys. Rev. Lett. **52**, 835 (1984).
[7] S. Komura, K. Osamura, H. Fujii, and T. Takeda, Phys. Rev. B **31**, 1278 (1985).
[8] M. Furusaka, Y. Ishikawa, and M. Mera, Phys. Rev. Lett. **54**, 2611 (1985).
[9] O. Lyon and J. P. Simon, Phys. Rev. B **35**, 5164 (1987).
[10] B. Rodmacq, M. Maret, J. Laugier, L. Billard, and A. Chamberod, Phys. Rev. B **38**, 1105 (1988).
[11] R. D. Lorentz, A. Bienenstock, and T. I. Morrison, Phys. Rev. B **49**, 3172 (1994).
[12] M. J. Regan and A. Bienenstock, Phys. Rev. B **51**, 12170 (1995).
[13] S. Mazumder, D. Sen, I. S. Batra, R. Tewari, G. K. Dey, S. Banerjee, A. Sequeira, H. Amenitsch, and S. Bernstorff, Phys. Rev. B **60**, 822 (1999).
[14] R. Tewari, S. Mazumder, I. S. Batra, G. K. Dey, and S. Banerjee, Acta Mater. **48**, 1187 (2000).
[15] D. Sen, S. Mazumder, R. Tewari, P. K. De, H. Amenitsch, and S. Bernstorff, J. Alloys Compd. **308**, 250 (2000).
[16] M. Kriechbaum, G. Degovics, J. Tritthart, and P. Laggner, Prog. Colloid Polym. Sci. **79**, 101 (1989).
[17] A. Heinemann, H. Hermann, K. Wetzig, F. Haeussler, H. Baumbach, and M. Kroening, J. Mater. Sci. Lett. **18**, 1413 (1999).
[18] R. A. Livingston, D. A. Neumann, A. J. Allen, S. A. Fitzgerald, and R. Berliner, Neutron News **11**, 18 (2000).
[19] C. V. Santilli, S. H. Pulcinelli, and A. F. Craievich, Phys. Rev. B **51**, 8801 (1995).
[20] A. Chakrabarti, R. Toral, J. D. Gunton, and M. Muthukumar, Phys. Rev. Lett. **63**, 2072 (1989).
[21] B. Dunweg and K. Kremer, Phys. Rev. Lett. **66**, 2996 (1991).
[22] M. Takenaka and T. Hashimoto, Phys. Rev. E **48**, R647 (1993).
[23] G. Brown and A. Chakrabarti, Phys. Rev. E **48**, 3705 (1993).
[24] G. Krausch, C. A. Dai, E. J. Kramer, and F. S. Bates, Phys. Rev. Lett. **71**, 3669 (1993).
[25] M. Rubinstein, R. H. Colby, and A. V. Dobrynin, Phys. Rev. Lett. **73**, 2776 (1994).
[26] S. Bastea and J. L. Lebowitz, Phys. Rev. Lett. **78**, 3499 (1997).
[27] W. R. White and P. Wiltzius, Phys. Rev. Lett. **75**, 3012 (1995).
[28] S. R. Shannon and T. C. Choy, Phys. Rev. Lett. **79**, 1455 (1997).
[29] P. W. Zhu, J. W. White, and J. E. Epperson, Phys. Rev. E **62**, 8234 (2000).
[30] E. Falck, O. Punkkinen, I. Vattulainen, and T. Ala-Nissila, Phys. Rev. E **68**, 050102(R) (2003).
[31] C. O. Kim and W. L. Johnson, Phys. Rev. B **23**, 143 (1981).
[32] A. F. Craievich and J. M. Sanchez, Phys. Rev. Lett. **47**, 1308 (1981).
[33] A. F. Craievich, J. M. Sanchez, and C. E. Williams, Phys. Rev. B **34**, 2762 (1986).
[34] S. Sen and J. F. Stebbins, Phys. Rev. B **50**, 822 (1994).
[35] A. Wiedenmann and Jun-Ming Liu, Solid State Commun. **100**, 331 (1996).
[36] A. Malik, A. R. Sandy, L. B. Lurio, G. B. Stephenson, S. G. J. Mochrie, I. McNulty, and M. Sutton, Phys. Rev. Lett. **81**, 5832 (1998).
[37] J. H. He and E. Ma, Phys. Rev. B **64**, 144206 (2001).
[38] A. Chakrabarti, Phys. Rev. Lett. **69**, 1548 (1992).
[39] J. C. Lee, Phys. Rev. B **46**, 8648 (1992).
[40] C. K. Chan, Phys. Rev. Lett. **72**, 2915 (1994).
[41] J. Jacob, A. Kumar, S. Asokan, D. Sen, R. Chitra, and S. Mazumder, Chem. Phys. Lett. **304**, 180 (1999).
[42] C. M. Knobler and N. C. Wong, J. Phys. Chem. **85**, 1972 (1981).
[43] Y. C. Chou and W. I. Goldburg, Phys. Rev. A **23**, 858 (1981).
[44] D. N. Sinha and J. K. Hoffer, Physica B & C **107**, 155 (1981).
[45] Benoit. B. Mandelbrot, *The Fractal Geometry of Nature* (Freeman, San Francisco, 1982).
[46] A. Guinier, G. Fournet, B. C. Walker, and L. K. Yudowith, *Small Angle Scattering of X-Rays* (Wiley, New York, 1955), pp. 167–195.
[47] O. Glatter and O. Kratky, *Small Angle X-Ray Scattering* (Academic Press, London, 1982).
[48] J. Tritthart and F. Haußler, Cem. Concr. Res. **33**, 1063 (2003).
[49] H. M. Jennings, Cem. Concr. Res. **30**, 101 (2000).
[50] D. Sen, T. Mahata, A. K. Patra, S. Mazumder, and B. P. Sharma, J. Phys.: Condens. Matter **16**, 6229 (2004).
[51] D. Sen, J. Bahadur, S. Mazumder, V. Bedekar, and A. K. Tyagi, J. Phys.: Condens. Matter **20**, 035103 (2008).
[52] J. Bahadur, D. Sen, S. Mazumder, R. Shukla, and A. K. Tyagi, J. Phys.: Condens. Matter **20**, 345201 (2008).
[53] D. Winslow, J. M. Bukowski, and J. Francis Young, Cem. Concr. Res. **25**, 147 (1995).
[54] T. A. Witten, Jr. and L. M. Sander, Phys. Rev. Lett. **47**, 1400 (1981).
[55] P. Meakin, Phys. Rev. Lett. **51**, 1119 (1983).
[56] M. Kolb, R. Botet, and R. Jullien, Phys. Rev. Lett. **51**, 1123 (1983).
[57] R. Thouy and R. Jullien, J. Phys. A **27**, 2953 (1994).
[58] R. Thouy and R. Jullien, J. Phys. I **6**, 1365 (1996).
[59] P. Meakin and F. Family, Phys. Rev. A **38**, 2110 (1988).
[60] S. Mazumder, Physica B **385-386**, 7 (2006).
[61] S. Mazumder, in *Neutron and X-Ray Scattering 2007: The International Conference*, edited by A. Ikram *et al.*, AIP Conf. Proc. No. 989 (AIP, New York, 2008), p. 29.
[62] J. Teixeira, J. Appl. Crystallogr. **21**, 781 (1988).
[63] T. Freltoft, J. K. Kjems, and S. K. Sinha, Phys. Rev. B **33**, 269 (1986).
[64] M. J. Vold, J. Colloid Sci. **14**, 168 (1959).
[65] P. Meakin, Phys. Rev. A **38**, 994 (1988).